

Structural and Dynamical Analysis of the Hydration of the Alzheimer's β -Amyloid Peptide

FRANCESCA MASSI, JOHN E. STRAUB

Department of Chemistry, Boston University, Boston, Massachusetts 02215

Received 17 September 2001; Accepted 5 March 2002

Abstract: An analysis of the water molecules in the first solvation shell obtained from the molecular dynamics simulation of the amyloid $\beta(10-35)\text{NH}_2$ peptide and the amyloid $\beta(10-35)\text{NH}_2\text{E22Q}$ "Dutch" mutant peptide is presented. The structure, energetics, and dynamics of water in the hydration shell have been investigated using a variety of measures, including the hydrogen bond network, the water residence times for all the peptide residues, the diffusion constant, experimentally determined HN amide proton exchange, and the transition probabilities for water to move from one residue to another or into the bulk. The results of the study indicate that: (1) the water molecules at the peptide-solvent interface are organized in an ordered structure similar for the two peptide systems but different from that of the bulk, (2) the peptide structure inhibits diffusion perpendicular to the peptide surface by a factor of 3 to 5 relative to diffusion parallel to the peptide surface, which is comparable to diffusion of bulk water, (3) water in the first solvation shell shows dynamical relaxation on fast (1–2 ps) and slow (10–40 ps) time scales, (4) a novel solvent relaxation master equation is shown to capture the details of the fast relaxation of water in the peptide's first solvation shell, (5) the interaction between the peptide and the solvent is stronger in the wild type than in the E22Q mutant peptide, in agreement with earlier results obtained from computer simulations [Massi, F.; Straub, J. E. *Biophys J* 2001, 81, 697] correlated with the observed enhanced activity of the E22Q mutant peptide.

© 2002 Wiley Periodicals, Inc. *J Comput Chem* 24: 143–153, 2003

Key words: A β -peptide; amyloid; E22Q "Dutch" mutant peptide; residence times; diffusion constant

Background

The amyloid β -peptide (A β -peptide) is currently the focus of one of the most widely accepted and well studied theories of the origin of Alzheimer's disease.² For this reason, the peptide has been the object of many experimental studies that have explored, with some success, its structure in solution and in the fibril, and its activity in the process of fibril growth. Although much progress has been made, a complete understanding of the mechanism of amyloid fibrillogenesis and fibril elongation remains an open question.

More than one possible hypothesis has been proposed for the process of fibril formation and elongation.^{3–6} One is based on the formation of nuclei from unstructured peptide monomers in solution.³ Once a nucleus reaches a certain size, fibrils grow by the addition of peptide monomers to the end of the growing fibrils.^{7,8} A second hypothesis is based on the formation of protofibrils of intermediate size that subsequently associate to form the full length fibril.^{9–11} Once formed, a fibril can grow by addition of peptide monomers to its end.^{12,13} The last hypothesis assumes the formation of micelles, by association of peptide monomers, which can convert into fibril nuclei upon reaching a critical size.^{3,7,8} A conclusive understanding of the

relative validity and importance of each of these hypotheses has not yet been reached.

It has been demonstrated that under certain conditions, pre-existing fibrils elongate by addition of peptide monomers at the fibrils' ends. This process follows a first order kinetics in the concentration of the monomeric peptide.^{10,12,13} There are two main pathways that have been proposed for this elongation process: transition of the monomer in solution to an activated configuration, similar to predominately β -form of the fibril aggregates, that can quickly deposit onto the plaque;^{14–17} absorption of the monomer in its solution configuration onto the plaque, followed by reorganization to a well-formed fibril.¹⁸ A recently proposed "energy landscape mechanism" considers both pathways, having two separate channels for this process, without making any *a priori* assumptions.¹⁹ Evidence suggests the predominance of the second pathway.

Correspondence to: J. E. Straub; e-mail: straub@bu.edu

Contract/grant sponsor: National Institutes of Health; contract/grant number: IR01 NS41356-01 (J.E.S.)

Contract/grant sponsor: National Science Foundation; contract/grant number: CHE-9975494 (J.E.S.)

The solution structure of the monomeric A β (10-35)-peptide congener has been experimentally determined by Lee and coworkers.²⁰ The structure, referred to as a collapsed coil (CC), is characterized by two key regions: a central hydrophobic cluster (CHC) (LVFFA) and a stable adjacent turn region (VGSN). This result proved that the structure of the monomeric peptide in aqueous solution is not α -helical, as was originally proposed based on the trifluoroethanol (TFE)-water structure, which showed that under those membrane-mimicking conditions the peptide consists of two short α -helical regions.²¹

The results of subsequent multiple nanosecond molecular dynamics calculation of the fully solvated A β (10-35)-peptide indicated that the collapsed coil configuration is maintained for the entire length of the simulation time, with fluctuations that were larger for the less structured N and C termini.²² Comparison of calculated and experimentally measured observables showed that the computational model was able to capture the structure and the dynamical behavior of the solvated peptide.

Experimental analysis of the E22Q “Dutch” mutant peptide proved that this peptide is significantly more active than the WT peptide, with a twofold increase in the rate of fibril elongation.²³ The exact nature of the increased activity of the E22Q mutant peptide relative to that of the WT peptide is still unclear, although different hypotheses have been considered.^{23–27} The structure of the monomeric E22Q mutant peptide in aqueous solution is still unknown and controversial. While CD experiments have shown evidence of β -structure,²⁶ NMR measurements of H $_{\alpha}$ proton chemical shifts indicate that the structure of the monomeric peptide in solution is indistinguishable from the CC structure of the WT peptide.²⁸

The results of multiple nanosecond molecular dynamics calculations of the fully solvated A β (10-35)NH $_2$ E22Q mutant peptide showed that it is also stable in a CC configuration similar to that of the WT peptide.¹ Comparing the results of the dynamics to those obtained for the WT peptide, some features were apparent: the structure of the E22Q mutant peptide presented larger fluctuations relative to the WT peptide; the mutant peptide’s structure is more open, with a larger solvent exposed surface area; the structure of the water in the first solvation shell is altered, resulting in a less attractive energy of interaction between the solvent molecules and the E22Q mutant peptide, relative to the WT peptide. These results suggest that in the process of deposition of the peptide onto the fibril, the desolvation step might be responsible for the different activity showed by these two peptide congeners. A more detailed analysis of the structural and dynamic properties of the solvent, with particular attention to the solvent-protein interface, is needed to explore the crucial role of the solvent in the process of aggregation, and to understand the influence of the peptide sequence.

It is well established that the water plays a very important role in determining the structure and activity of peptides and proteins in aqueous solution. Different experimental techniques have been employed to understand the properties of the water in proximity to the protein surface, among them NMR,^{29,30} Raman³¹ and IR^{32,33} spectroscopies, X-ray and neutron diffraction crystallography,^{34–36} Brillouin scattering,³⁷ and inelastic and quasielastic neutron scattering.^{38,39} Although each technique gives important information about the relaxation time and energetics of the water molecules at the interface with the protein, the results may be

contradictory due to different resolution times among them. Computer simulation represents a very powerful tool for the study of the structure and the dynamics at the protein-solvent interface at the atomic level.

In this article, we present an analysis of the water molecules in the first solvation shell obtained from the molecular dynamics simulation of the A β (10-35)NH $_2$ peptide and of the A β (10-35)NH $_2$ E22Q mutant peptide. In order to study the water mobility around these peptides, we calculated the water residence times in the first solvation shell. In particular, we considered a relaxation time that corresponds to the average time a water molecule spends in the solvation shell of a given peptide atom. We also calculated the diffusion constant for lateral diffusion of water along the peptide surface and compared our computed result with the diffusion constant of bulk water. To understand the structure and the nature of the protein-solvent interactions, we analyzed the hydrogen bonds that each peptide residue forms with the solvent and internally. Finally, a master equation model was developed to study the kinetics of water diffusion along the peptide surface. This type of analysis allowed us to predict the distribution of water molecules in the first solvation shell and to characterize the dominant features of the solvent relaxation process for the WT and for the Dutch mutant peptides.

Methods

The initial conditions for our simulations of the wild-type β (10-35)-NH $_2$ peptide and the E22Q mutant peptide were derived from the NMR solution structure of Lee and coworkers²⁰ derived from distance geometry calculations employing NMR derived NOE restraints. The structure of the E22Q mutant peptide was modeled from the wild-type structure. Currently, there is no NMR derived structure of the E22Q mutant peptide analogous to the structure of the WT A β (10-35)-peptide congener. However, NMR measurements of H $_{\alpha}$ proton chemical shifts for the WT and E22Q mutant A β (10-35)-peptides are consistent with a structure of the E22Q mutant that is indistinguishable from the known structure of the WT peptide.²⁸ In this section, after a brief description of the simulation model and protocol, details on the methods used to calculate the water residence times, the hydrogen bond network between solvent and peptide, the water lateral diffusion constant, and the solvent relaxation master equation transition matrix are provided.

Simulation Model and Protocol

For the fully solvated wild-type and mutant peptides, four independent 1 ns trajectories were simulated. Each trajectory originated from one of a set of four initial peptide structures that were chosen from two families of conformers characterized by variations in their C-terminal regions. The initial structures resulted from the work of Lee and coworkers,^{20,22,28,40} who used a combination of distance geometry refinement and molecular dynamics annealing/minimization procedures employing experimentally derived NOE restraints. The core regions of the peptide, including the LVFFA and VGSN substructures, were largely similar in the four starting configurations. However, outside of that core of the

structure there was significant disorder in the N- and C-terminal regions of the peptide due to the small number of experimentally derived restraints in those regions.

The simulation protocol, summarized below, has been described elsewhere in detail.^{1,22} For the simulations of the wild-type and mutant peptides, the solute was centered in a rhombic dodecahedron cell that was carved from a cubic box of 50 Å on a side and filled with 2113 water molecules. Periodic boundary conditions were applied to avoid edge effects. The energetics of the A β peptide in water were simulated using the version 22 potential energy function of the CHARMM program.⁴¹ Nonbonded interactions were truncated at 12.0 Å and Ewald summation was used to evaluate the electrostatic interactions. The SHAKE algorithm was employed to constrain bonds involving hydrogen atoms to their equilibrium values. A time step of integration of 2 fs was employed in the Verlet algorithm in the CHARMM program.⁴² After an equilibration period of 200 ps, a production run of 1 ns was completed with an average temperature of 300K. Every 200 fs, coordinates and energetic data were collected.

Water Residence Times

We have analyzed the residence times of solvent molecules surrounding the peptide. The first coordination shell was defined as a shell of radius equal to 4 Å around each atom of the protein. For every protein atom, α , we calculated the “survival function” $P_\alpha(t)$,^{43,44} defined as

$$P_\alpha(t) = \sum_{j=1}^{N_w} \frac{1}{T_{\text{run}} - t + 1} \sum_{t_0}^{T_{\text{run}} - t_0} p_{\alpha,j}(t_0, t_0 + t) \quad (1)$$

where $p_{\alpha,j}(t_0, t_0 + t)$, the “survival probability function,” is a binary function that takes the value of 1 if the j th water molecule has remained in the coordination shell of atom α from t_0 to $t_0 + t$; otherwise the function is equal to zero. N_w is the total number of water molecules; T_{run} is the length of the simulation. The “survival function” represents the average number of water molecules that remain in the coordination shell of atom α for a time t . From this function it is possible to evaluate a relaxation time τ through a single exponential fitting of $P_\alpha(t)$ as

$$\ln P_\alpha(t) = \ln P_\alpha(0) - \frac{t}{\tau} \quad (2)$$

where τ is the average time that a water molecule spends inside the hydration shell of peptide atom α .

We have used a second approach to evaluate the residence times of water molecules around the peptide atom α . The mean residence time was defined⁴⁵ as

$$\tau_{\text{mean}}(\alpha) = \frac{1}{N_w} \sum_{j=1}^{N_w} \tau_j(\alpha) \quad (3)$$

with N_w equal to the number of water molecules visiting atom α during the entire simulation time, and $\tau_j(\alpha)$ is equal to the value of

the residence time of the water molecule j in the hydration shell of protein atom α .

Hydrogen Bond Analysis

Every saved configuration was analyzed for protein-water hydrogen bonding. We used the following definition to identify the presence of a hydrogen bond: the distance between the donor-acceptor pair was required to be less than or equal to 2.5 Å, and the angle between the donor and acceptor diatomic groups was required to be between 113–180°. ⁴⁶ The hydrogen bonding frequency was estimated by dividing the number of snapshots (instantaneous configurations) showing hydrogen bonds by the total number of snapshots examined for the entire simulation.

Diffusion of Water in the Peptide's First Solvation Shell

The mean-square displacement of the oxygen atoms of water molecules surrounding the peptide, $\Delta r_o(t)^2$, was computed as a function of time as

$$\langle \Delta r_o(t)^2 \rangle = \frac{1}{N_w} \sum_{j=1}^{N_w} \frac{1}{T_{\text{run}} - t + 1} \sum_{t_0}^{T_{\text{run}} - t_0} [r_o(t + t_0) - r_o(t_0)]^2 \quad (4)$$

At each t_0 we labeled the water molecules residing inside the first hydration shell of the peptide. N_w is the number of water molecules inside the hydration shell at t_0 , which remained so until $t_0 + t$. It is only these N_w water molecules that contribute to the sum appearing in Eq. (4). The diffusion constant of water in the first solvation shell of the peptide was estimated using the Einstein relation:^{45,47–50}

$$\langle \Delta r_o(t)^2 \rangle \sim 6Dt \quad (5)$$

We also decomposed the overall diffusion constant of the solvent moving in the first solvation shell of the peptide into components parallel and perpendicular to the peptide surface:^{49,51}

$$\langle \Delta r_{\parallel o}(t)^2 \rangle \sim 4D_{\parallel}t \quad (6)$$

$$\langle \Delta r_{\perp o}(t)^2 \rangle \sim 2D_{\perp}t \quad (7)$$

where Δr_{\parallel} and Δr_{\perp} are parallel and perpendicular displacements from the peptide surface, respectively. Figure 1 shows the decomposition of the displacement vector in the perpendicular and parallel components. For the positions A (at time t_0) and B (at time $t_0 + t$) of each water molecule, the closest peptide atoms, C and D, respectively, were identified. The perpendicular and parallel displacements were calculated as

$$\Delta r_{\perp o}(t) = |\mathbf{DB}| - |\mathbf{CA}| = |\mathbf{DB}| - |\mathbf{DA}'| \quad (8)$$

$$\Delta r_{\parallel o}(t) = |\mathbf{AA}'| = |\mathbf{AB} - \mathbf{A'B}| \quad (9)$$

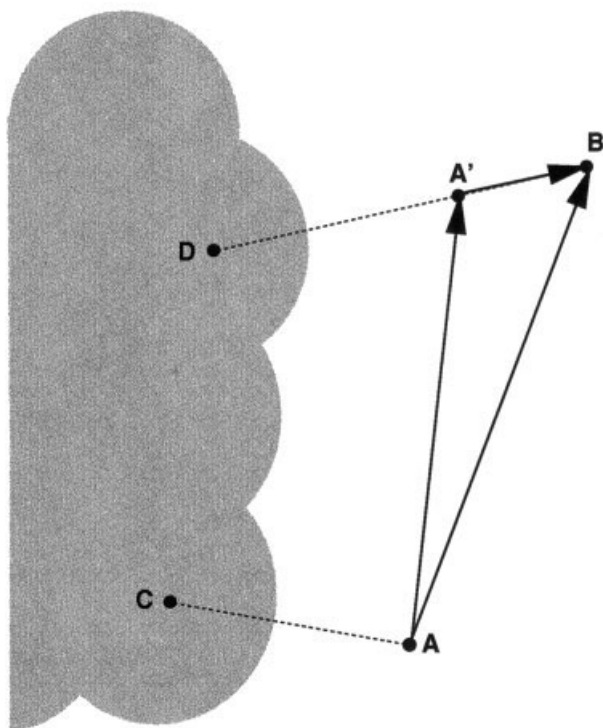


Figure 1. Decomposition of the solvent displacement into parallel and perpendicular components, based upon Figure 1 of Makarov et al.⁵¹

Transition Matrix

In order to study the dynamics of the water molecules in the peptide's first hydration shell, we considered their positions, relative to the different residues of the peptide, as a function of time. We were particularly interested in studying the kinetics of the transitions of water molecules from the solvation shell of one peptide site to another, or to the bulk. The rate constant of transition from site i to site j along the peptide, k_{ji} , was defined as equal to the inverse of the average time, τ_{ji} , spent by water molecules around position i before moving to position j , where positions i, j were taken to be the hydration shells of any peptide residue or the bulk. Having so calculated k_{ji} , the rate constant for the transitions from residue site i into the bulk, detailed balance was used to determine the rate constant for the inverse process.⁵² The average time τ_{ji} was calculated for every i, j for each trajectory. This allowed us to build a transition matrix \mathbf{W} whose elements were defined as^{52,53}

$$\mathbf{W}_{ij} = k_{ij} - \delta_{ij} \left(\sum_k k_{ki} \right) \quad (10)$$

By construction, the following properties characterize the matrix \mathbf{W} : $\mathbf{W}_{ij} \geq 0$ for $i \neq j$, $\sum_i \mathbf{W}_{ij} = 0$. For a closed system, where the total number of water molecules is constant, the sum of each column of \mathbf{W} must be equal to zero. The master equation that

describes the flux of water molecules along the surface of the peptide as a function of time^{52–54} can be written as

$$\frac{d\mathbf{p}(t)}{dt} = -\mathbf{W}\mathbf{p}(t) \quad (11)$$

where $p_i(t)$, the i th component of the vector $\mathbf{p}(t)$, represents the probability of finding a water molecule in the hydration shell of site i at time t . The evolution of the probabilities $p_i(t)$ is given by the solution to eq. (11):

$$\mathbf{p}(t) = \mathbf{p}^{\text{eq}} + \sum_{E_i < 0} C_i \mathbf{s}_i e^{-E_i t} \quad (12)$$

where \mathbf{s}_i are the eigenvectors of \mathbf{W} and E_i the corresponding eigenvalues; \mathbf{p}^{eq} is the eigenvector representing the probabilities at equilibrium; and corresponding to $E_i = 0$; C_i are the coefficients determined by the initial distribution of probabilities $\mathbf{p}(0)$.

Results and Discussion

In this section we present the results of our simulations and analysis.

Water Residence Time

The mean residence time τ_i has been evaluated from a single exponential fitting of the survival probability function. In Figure 2 the survival probability function $P_\alpha(t)$ is presented as a function of time. It appears that the decay of the survival probability function cannot be represented by a single exponential. The general behavior of $P_\alpha(t)$ can be clearly decomposed into three different regions: initial fast decay for times smaller than 2 ps, exponential decay for times between 2 and 20 ps, and faster than exponential decay for longer times, when very few water molecules remain around the peptide atom. The initial fast decay can be reasonably attributed to those water molecules that recross the solvation shell

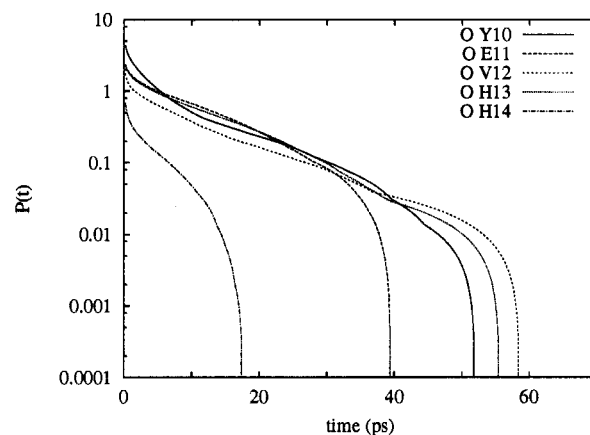


Figure 2. The survival probability function $P_\alpha(t)$ of different backbone oxygen atoms is plotted as a function of time.

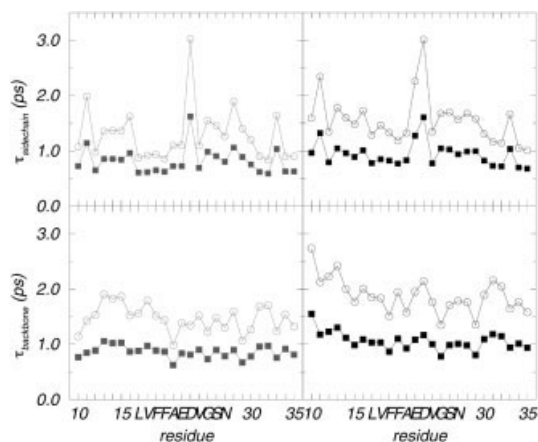


Figure 3. Time constants, obtained by fitting the initial fast decay of the survival probability function as a single exponential process, are compared with the mean residence time, calculated using eq. (3). The results have been averaged for the backbone atoms and for the sidechain atoms over all trajectories. The fitted values of the time constant are represented as empty circles, the mean residence times are filled squares. The results obtained for the WT peptide are presented in black, those of the E22Q mutant peptide in gray.

boundary of the peptide. The fast decay should therefore depend upon the definition of the solvation shell. To find the time scale for this recrossing process, we fitted the initial fast decay of the survival probability function with a single exponential. The time constants found for this fast decay are of the same order of magnitude, and have the same behavior when plotted as a function of the peptide atom, as the residence times calculated using the approach suggested by Muegge and Knapp.⁴⁵

The time constants for the initial fast decay of $P_{\alpha}(t)$ are presented in Figure 3. When we fitted the survival probability function with a double exponential, with two different sets of decay times, τ_f (fast) and τ_s (slow), we obtained relatively good agreement for times between 0 and 20 ps. Two examples are shown in Figure 4. These results suggest that the residence times calculated using eq. (3)⁴⁵ are strongly influenced by the rapid recrossing process of the solvation shell. The values of τ_f used are the residence times calculated with eq. (3). The values of τ_s are derived by fitting the central region of the survival probability function. The values of τ_f and τ_s for the backbone atoms are presented in Table 1. The general trend that was found for the water residence time as a function of the polar/nonpolar nature of the peptide atom agrees with earlier work on different systems^{43,44}: $\tau_{\text{charged}} > \tau_{\text{polar}} > \tau_{\text{nonpolar}}$. In Table 1, to demonstrate the range of values of τ_f and τ_s , the minimum and maximum values for a given atom type are listed in bold.

To compare the results obtained from the simulation of the WT and E22Q mutant peptides, we considered the average values of the water residence times of the backbone and sidechain atoms. In Figure 5 we plot the values of the mean residence time, τ_s , which has been evaluated from a single exponential fitting of the central part of the survival probability function. The water residence time around the sidechain atoms at position 22 is higher in the WT than in E22Q mutant peptide, consistent with the fact that in the WT,

residue 22 is charged while in the mutant it is polar. We observe a similar trend if τ_f [from eq. (3)] is examined. The comparison of Figure 5 with Figure 6 shows that there is a correlation between the water residence time and the solvent exposed surface area, indicating that those residues that are more exposed to the solvent also have higher values of the water residence time. The water residence times of the WT peptide are consistently higher than those of the E22Q mutant, indicating that the interactions between the peptide atoms and the water molecules are stronger in the WT than in the mutant congener. This result is in agreement with the data obtained from the analysis of the energy of interaction of the peptide with the solvent molecules in the first solvation shell,¹ summarized in Figure 7. The energy of interaction of the water molecules in the first solvation shell is more negative (more attractive) for the WT than for the mutant peptide, leading to longer water residence times around the atoms of the WT than those of the E22Q mutant peptide. The only exception is found in the backbone atoms of residue 15–19 where the opposite is true. As Figure 9 shows, the residues of the WT peptide in this region have a higher probability of being involved in an intramolecular hydrogen bond than those of the E22Q mutant; consequently they are less likely form a hydrogen bond with the solvent.

Diffusion of Water in the Peptide's First Solvation Shell

The lateral diffusion of the water along the surface of the peptide was computed using the Einstein relation for the mean-square displacement of water oxygen atoms. The values of the overall diffusion constant resulting from each of the four trajectories were averaged to obtain $D_{\text{WT}} = (0.15 \pm 0.05) \text{ \AA}^2\text{ps}^{-1}$ and $D_{\text{E22Q}} = (0.17 \pm 0.02) \text{ \AA}^2\text{ps}^{-1}$, for the WT and E22Q mutant peptides, respectively. From the decomposition of the overall diffusion constant into components parallel and perpendicular to the peptide surface, we found the average values of D_{\parallel} and D_{\perp} for the WT and the E22Q mutant. The results are presented in Table 2.

The results obtained from the analysis of the two peptide systems do not present significant differences. These results indi-

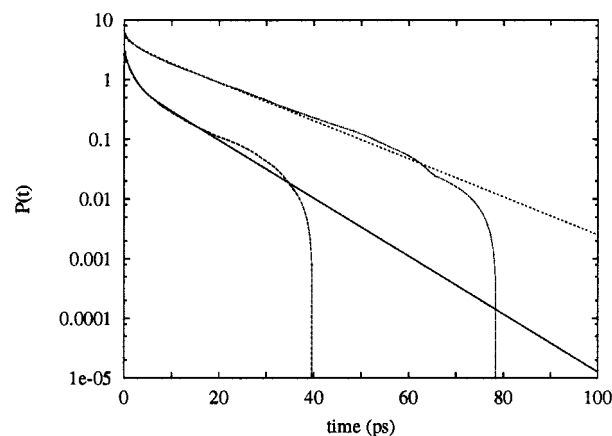


Figure 4. The result of the double exponential fit of the survival probability function of the backbone N atom and of the sidechain C $_{\gamma}$ atom of Tyr10.

Table 1. Water Residence Times.

Residue	WT						E22Q					
	O		H		C_{α}		O		H		C_{α}	
	τ_s	τ_f	τ_s	τ_f	τ_s	τ_f	τ_s	τ_f	τ_s	τ_f	τ_s	τ_f
10	8.8	1.2	14.4	1.4	9.8	1.9	5.8	1.1	1.3	0.69	1.4	0.44
11	12.3	1.6	13.0	1.2	12.3	0.82	5.4	1.1	10.4	0.91	1.6	0.51
12	11.0	1.2	10.9	1.2	10.3	0.91	9.1	1.1	13.8	1.0	2.2	0.55
13	13.1	1.1	31.8	1.5	11.5	0.97	20.1	1.2	20.9	1.2	2.9	0.66
14	8.0	1.1	13.6	1.2	9.5	0.80	7.2	0.89	30.9	1.2	3.3	0.68
15	11.5	1.3	11.1	1.1	11.1	0.71	7.2	1.2	56.2	1.1	2.9	0.57
16	21.2	1.5	17.9	1.5	8.3	0.64	13.3	1.1	38.9	1.1	3.1	0.56
17	12.5	1.5	8.2	1.1	5.0	0.68	8.7	1.3	26.6	0.96	2.4	0.48
18	15.5	1.3	16.2	0.87	6.8	0.88	39.3	1.4	28.9	0.93	2.4	0.59
19	3.8	0.6	7.2	0.89	5.6	0.59	12.0	1.3	8.3	0.66	1.7	0.59
20	7.6	1.0	7.2	1.6	8.2	0.75	6.1	1.1	5.9	1.5	1.0	0.40
21	8.0	1.0	9.1	0.95	7.6	0.68	10.5	0.83	6.2	0.49	2.3	0.51
22	11.1	1.3	17.4	1.2	12.9	0.76	4.9	1.0	8.3	0.89	1.6	0.54
23	8.9	1.5	14.5	0.95	11.7	0.75	5.1	1.2	12.4	0.73	2.1	0.53
24	9.7	1.2	6.0	1.35	10.6	0.80	4.8	1.1	12.5	1.8	1.1	0.43
25	10.1	1.1	10.4	0.72	11.1	0.71	8.6	1.1	24.5	0.74	1.8	0.62
26	8.9	1.3	7.5	0.97	8.3	0.70	8.7	1.1	8.7	1.0	1.3	0.53
27	9.5	1.1	10.2	0.80	9.2	0.84	7.6	0.93	9.0	0.76	2.2	0.58
28	8.4	1.1	23.0	1.2	6.5	0.61	5.7	1.1	15.8	1.1	2.5	0.43
29	12.3	1.0	13.3	0.88	5.2	0.68	9.2	1.1	14.4	0.61	1.2	0.55
30	8.7	1.3	8.1	1.0	9.8	0.65	9.0	1.1	4.2	0.64	1.5	0.54
31	10.0	1.3	38.3	1.5	9.7	0.85	6.2	1.2	21.6	1.2	2.4	0.60
32	21.0	1.1	18.0	1.3	8.7	0.77	11.0	1.2	18.6	1.2	1.7	0.57
33	8.7	1.0	14.4	1.2	8.7	0.71	7.2	0.87	7.1	0.93	2.3	0.67
34	18.1	1.4	13.9	1.0	6.9	0.68	6.5	1.2	10.1	0.93	2.6	0.51
35	7.2	1.0	20.2	1.2	7.4	0.60	4.4	0.89	2.7	0.90	1.3	0.48

cate that the overall diffusion of water molecules along the surface of the peptide is similar in the two peptide systems. The experimentally measured value of the diffusion constant of bulk water is equal to $0.23 \text{ \AA}^2 \text{ ps}^{-1}$.^{45,55} From our simulation, we find that the overall diffusion of water in the first solvation shell of the peptide is slower than that of bulk water. This effect has been observed in previous molecular dynamics simulations.^{49–51,56,57} We also observe that the diffusion rates in directions parallel and perpendicular to the surface of the peptide are, respectively, faster and slower than the overall diffusion rate. A similar effect has been observed in previous MD simulations of proteins in aqueous solution.⁵¹ The parallel component of the diffusion constant is similar to that of bulk water, while the perpendicular component is consistently smaller. An interpretation of these observations has been given previously:⁵¹ the perpendicular diffusion rate is decreased by the presence of a larger solute, which moves at a lower rate, and which also has an effect in reducing the dimensionality of space available to the solvent.

The surface of the peptide that is exposed to the solvent is very hydrophobic (see Fig. 6). The peptide is rich in hydrophobic residues that cannot form hydrogen bonds with the solvent. The reduced mobility of water in the first solvation shell of the peptide, relative to that of bulk water, could also be related to the organization of the solvent around the peptide in an ordered solvation

shell with a structure that is different from that of the bulk water.^{50,58}

We calculated the diffusion constant of water in the first solvation shell of different types of peptide atoms. In particular, the atoms were classified as being apolar, polar, or charged. The results are presented in Tables 3 and 4. The values of the overall diffusion constants are similar for charged atoms and apolar atoms; the diffusion constants for water near polar atoms tend to be highest. This result is in agreement with what was found in earlier simulations of globular proteins.^{50,58} This can be interpreted as a result of the more ordered structure of the solvation shell around apolar and charged atoms relative to that around polar atoms. The parallel component of the diffusion constant is always higher than the overall diffusion constant, while the perpendicular component is always smaller by approximately a factor of 5.

In the WT peptide, the ratio of D_{\parallel} to D_{\perp} is approximately two times greater than that for the E22Q mutant peptide. This result can be interpreted considering the different energies of interaction of the two peptide systems with the solvent, shown in Figure 7. The more attractive energy of interaction of the WT peptide with the solvent, relative to that of the E22Q mutant peptide, has a pronounced effect on the perpendicular component as a result of an increased energetic barrier, in the wild-type peptide, to motion perpendicular to the peptide surface. The diminished rate corre-

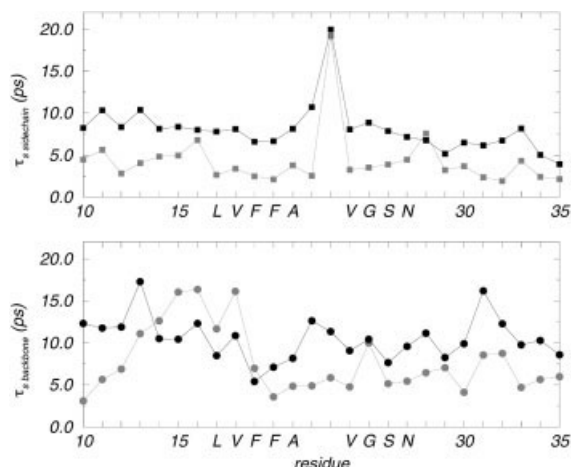


Figure 5. The water residence times of the atoms of the peptides have been averaged for the backbone atoms and for the sidechain atoms over all trajectories. The results obtained for the WT peptide are presented in black, those of the E22Q mutant peptide in gray.

sponds to a difference of roughly $k_B T/2$ in the average water-peptide atom interaction between the WT and mutant peptides.

Hydrogen Bond Analysis

The probability of formation of hydrogen bonds between the peptide and the solvent along the trajectories is depicted in Figure 8. The result shows that the hydrogen bond network between the solvent and the peptide is generally similar for both the mutant and wild-type peptides. The major differences in the results for the WT and the E22Q mutant peptide are found in the central region of the peptide. From residue 17 to residue 26, the average number of hydrogen bonds formed by the E22Q mutant peptide is higher than that of the WT peptide for every residue in this region, with the only exception being A21. Previous results obtained from the

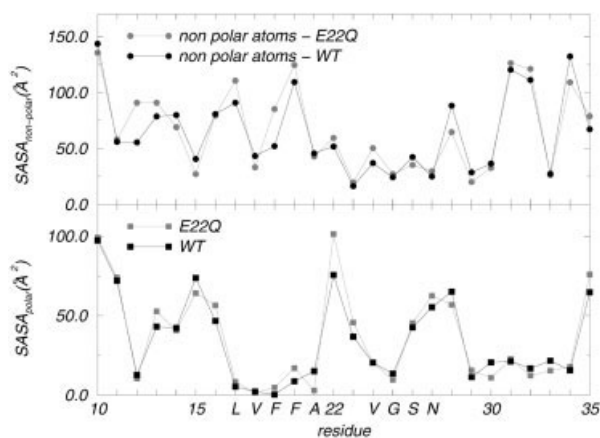


Figure 6. The solvent accessible surface area (SASA) of each residue of the peptide. The value of the SASA has been decomposed in two contributions, of polar and of nonpolar atoms.

Table 2. Average Values of the Diffusion Constant.

	D ($\text{\AA}^2\text{ps}^{-1}$)	D_{\parallel} ($\text{\AA}^2\text{ps}^{-1}$)	D_{\perp} ($\text{\AA}^2\text{ps}^{-1}$)
WT	0.17 ± 0.02	0.27 ± 0.02	0.05 ± 0.02
E22Q	0.15 ± 0.05	0.24 ± 0.05	0.07 ± 0.07

analysis of the MD trajectories of these two peptides indicated that the E22Q mutant congener has a higher solvent exposed surface area than the WT peptide.¹ Figure 6 shows the different contributions of polar and nonpolar atoms that are exposed to the solvent. Apart from A21, the E22Q mutant peptide has higher polar and nonpolar solvent accessible surface area in region 17–26. This can account for the higher average number of hydrogen bonds found in the simulation of the E22Q mutant relative to the WT peptide. As an interesting comparison we considered the probability of a given residue being involved in an intramolecular hydrogen bond along the trajectory. The results presented in Figure 9 indicate that the WT peptide has a consistently higher probability to form intramolecular hydrogen bonds relative to the E22Q mutant peptide in the same region (17–26) that presents a lower probability of forming hydrogen bonds with the solvent. This result is consistent with previous results that indicated that the E22Q mutant peptide structure in solution is more flexible.^{1,59}

In Figure 10 the values of the NH exchange rates, measured by Lee and coworkers,^{20,28,59} for all residues between K16 and N27 are represented together with the probability of formation of hydrogen bonds with the solvent. The pattern of the relatively uniform rate of exchange in this segment of the peptide is similar in form to that found for the probability of hydrogen bond formation with the solvent. However, it should be noted that the time scale for the process of amide hydrogen exchange with the solvent is on the order of 1 s, much longer than the time of our simulations (1 ns). For this reason, we do not expect to be able to capture, in these simulations, all the aspects of the dynamics of the peptide-solvent interaction that are crucial in determining the rate in the amide proton exchange process.

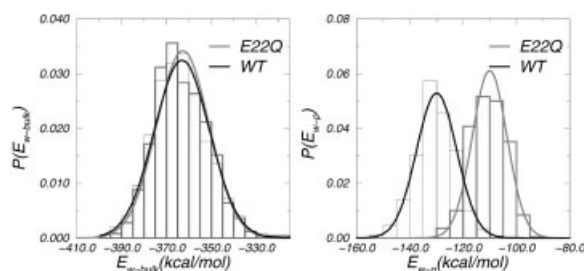


Figure 7. The average binding energy for water molecules in the first solvation shell of the peptide is decomposed in the two contributions E_{w-p} and E_{w-bulk} .^{62–64} E_{w-p} is the interaction of the proximal water molecules (w) with the peptide (p); E_{w-bulk} is the energy of interaction of the proximal water molecules with all the other water molecules in the system (bulk).

Table 3. WT Peptide's Average Values of the Diffusion Constant for Different Types of Atoms.

	WT		
	D ($\text{\AA}^2\text{ps}^{-1}$)	D_{\parallel} ($\text{\AA}^2\text{ps}^{-1}$)	D_{\perp} ($\text{\AA}^2\text{ps}^{-1}$)
Apolar atoms	0.16 ± 0.02	0.26 ± 0.02	0.05 ± 0.02
Polar atoms	0.17 ± 0.02	0.26 ± 0.02	0.05 ± 0.02
Charged atoms	0.16 ± 0.02	0.26 ± 0.02	0.06 ± 0.03

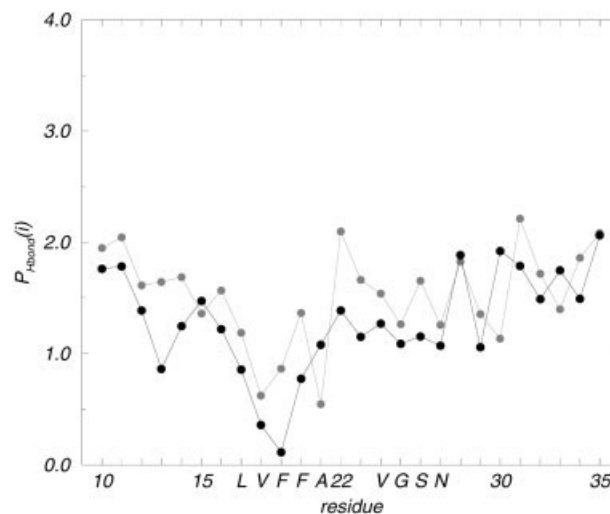
Transition Probabilities

Figure 11 shows the transition probabilities to move from residue j to residue i , k_{ij} , averaged over the four trajectories for the WT and the Dutch mutant peptide. The plot is not symmetric; k_{ij} is in general different from k_{ji} . From a first analysis of the plots, some differences between the two systems appear evident. The WT peptide presents exchange of water molecules between the N-terminus and C-terminus, and vice versa, that is absent in the E22Q mutant congener. The rates of transition from the N-terminus to the central core of the peptide (residue 19–28) have lower or zero values in the Dutch mutant than in the WT peptide. These features are common to both systems: a high rate of transition from residue D23 to N27 and from residue 22 to K28; transitions occur in the core, within the LVFFA region, and between VGSN and C-terminus regions. The plots obtained from each trajectory show an interesting correlation with the plots obtained from the cross-correlation calculations over the trajectories.¹ This result indicates that the probability of transition for water molecules is high between those regions whose coordinate fluctuations are correlated; that is, for those regions of the peptide that are often in close proximity, allowing water molecules to move between solvation shells.

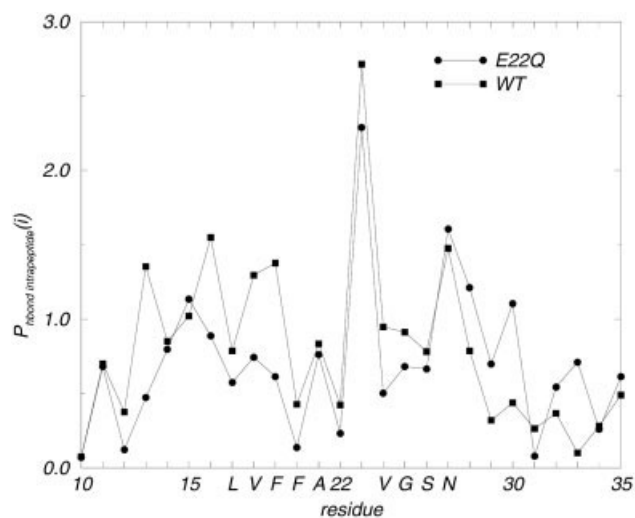
The solution of the master equation, given in eq. (11), allowed us to make a qualitative and quantitative analysis of the kinetics of the flux of the water molecules along the surface of the peptide. The eigenvalues of the transition matrix, \mathbf{W} , whose elements are defined in eq. (10), are presented in Figure 12. The analysis of Figure 12 shows some interesting features common to both peptides. There is always an eigenvalue that is equal to zero, corresponding to the system at equilibrium. The next eigenvalue, in increasing magnitude, has a value equal to 1.24 ps^{-1} for the WT peptide and equal to 1.29 ps^{-1} for the E22Q mutant peptide. This time scale is of the same order of magnitude as that of the process

Table 4. E22Q Mutant Peptide's Average Values of the Diffusion Constant for Different Types of Atoms.

	E22Q		
	D ($\text{\AA}^2\text{ps}^{-1}$)	D_{\parallel} ($\text{\AA}^2\text{ps}^{-1}$)	D_{\perp} ($\text{\AA}^2\text{ps}^{-1}$)
Apolar atoms	0.14 ± 0.05	0.2 ± 0.1	0.06 ± 0.05
Polar atoms	0.17 ± 0.08	0.3 ± 0.3	0.1 ± 0.1
Charged atoms	0.15 ± 0.03	0.23 ± 0.08	0.05 ± 0.03

**Figure 8.** The probability of formation of hydrogen bonds with the solvent as a function of the residue number of the amyloid peptide WT and E22Q mutant congeners. The results obtained from the simulation of the WT peptide are presented in black, those of the E22Q mutant peptide in gray.

of rapid recrossing of the solvation shell, which we determined from the first fast decay of the survival probability function. All the other eigenvalues have absolute values significantly larger than this one. Ten of the eigenvalues for the WT peptide and eight for the Dutch mutant peptide are complex. The imaginary part of the eigenvalue is always much smaller in magnitude relative to the real part. The presence of complex eigenvalues indicates that there is an oscillatory behavior of $p_i(t)$ as a function of time. The time scale of the imaginary part that determines the oscillatory behavior

**Figure 9.** The probability of intramolecular hydrogen bonds as a function of the residue number of the amyloid peptide, WT, and E22Q mutant congeners.

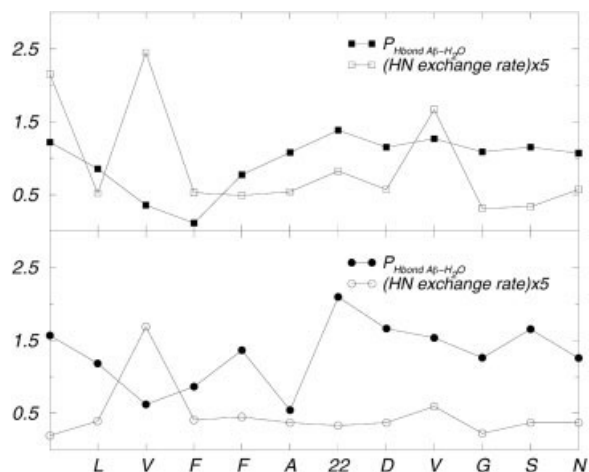


Figure 10. The probability of formation of hydrogen bonds with the solvent and the HN exchange rate as a function of the residue number for residues 16–27 of the amyloid peptide, WT, and E22Q mutant congeners. The results obtained from the simulation of the WT peptide are presented as squares, those of the E22Q mutant peptide as circles.

can be attributed to the process of rapid recrossing of water molecules that are at the boundary of the solvation shell.

Figure 13 presents the equilibrium probability distribution for water molecules around residues of the peptide, and compares results obtained directly from the simulation with those obtained from the solution of the master equation. Good qualitative agreement is observed between the two distributions. The solution of eq. (12) provides the time evolution of $p_i(t)$, the probabilities of finding water molecules at site i , where i can be a residue of the peptide or bulk water. Starting from different initial probability distributions, $\mathbf{p}(0)$, we could follow the evolution in time of $\mathbf{p}(t)$. Figure 14 shows the time evolution of the water probability to be

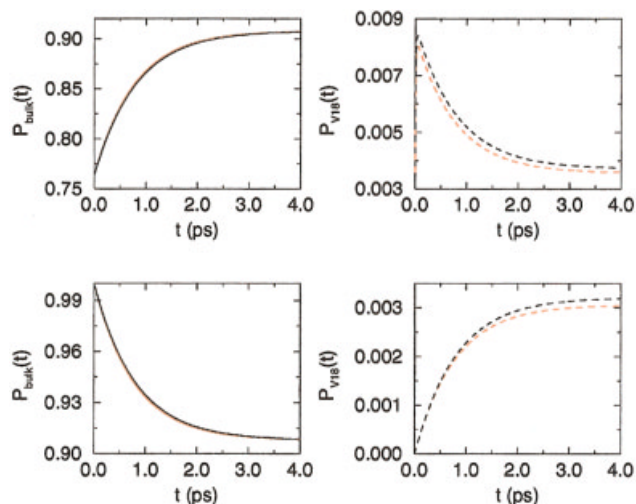


Figure 14. Time evolution of the probability distribution of water molecules in the bulk (solid line on the left hand side) and in the solvation shell of residue V18 (dashed line on right hand side) for the WT (black line) and for the E22Q mutant peptide (red line) starting from two different initial distributions. Five hundred fifty water molecules are initially in the first solvation shell of the peptide, and 1563 water molecules are in the bulk. The probability of being around residue i is equal to the ratio of the average solvent accessible surface area of that residue, $SASA_i$, over the average total solvent exposed surface area of the peptide $SASA_{tot}$, represented in the two plots on top. All the water molecules are initially in the bulk, represented in the two plots at the bottom.

in the bulk and in the solvation shell of residue V18, for two different initial configurations.

The plot of $P_{V18}(t)$ in the upper panel shows an initial rapid rise to a maximum value, followed by a decay until the equilibrium

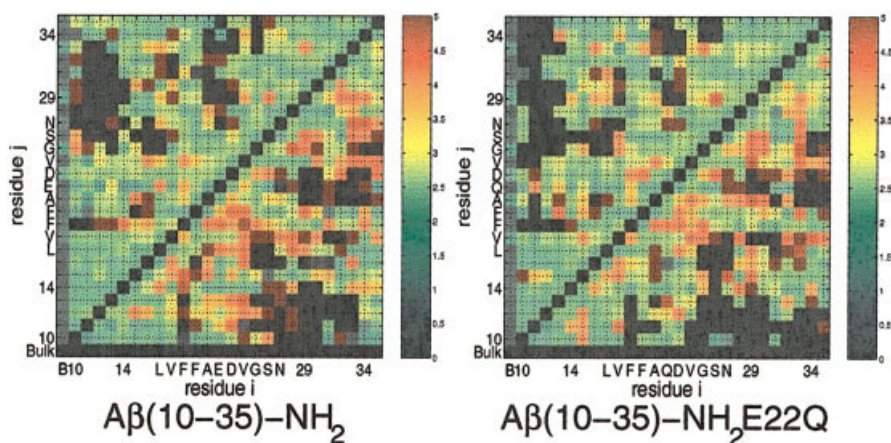


Figure 11. Water transition probabilities to move from site j to site i , and to the bulk. The plot shows the results averaged over all trajectories for the WT peptide, on the left, and for the E22Q mutant peptide, on the right. Red corresponds to a high probability to move from site j to site i , while blue corresponds to a low probability.

value is reached after about 3 ps. This ringing behavior is due to the presence of complex eigenvalues following rapid recrossing of the site boundaries. The same ringing behavior is observed for most of the amino acids in the central core region of the peptide and for residues 30 and 33.

Summary and Conclusions

All atom molecular dynamics simulations of the WT and E22Q mutant $\alpha\beta(10-35)\text{NH}_2$ peptide congeners were computed with the intent of gaining some insight into the crucial role of the solvent in the process of peptide aggregation and desolvation, and on the effect of the peptide sequence. We analyzed the structure and dynamics of the water molecules at the interface with the peptide. The results of our simulations support a number of conclusions.

1. The residence times of the WT peptide are consistently higher than those of the E22Q mutant peptide, indicating that the interaction between the peptide and the solvent is stronger in the WT than in the mutant congener, in agreement with earlier results obtained from computer simulations.¹ The general trend that was found for the water residence time as a function of the polar/nonpolar nature of a given peptide atom was $\tau_{\text{charged}} > \tau_{\text{polar}} > \tau_{\text{nonpolar}}$. Our results are consistent with earlier works on globular protein systems.^{43,44}
2. The diffusion constant of water molecules at the solvent-peptide interface is similar in the two $\alpha\beta$ -peptide congeners, and it is smaller than the diffusion constant of bulk water. These results indicate that the water molecules at the interface with the peptide are organized in an ordered solvation shell with a structure that differs from that of the bulk. This result is

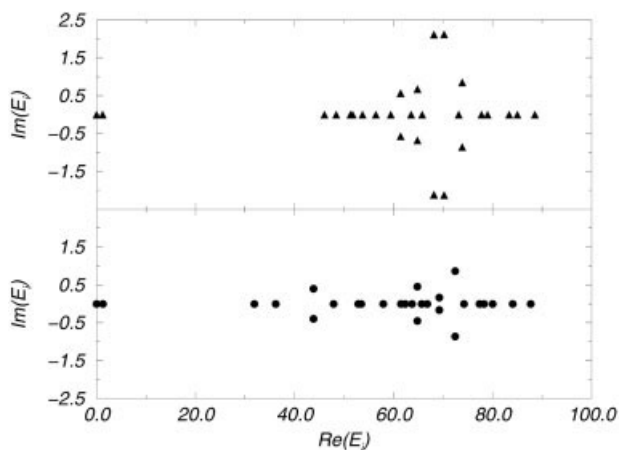


Figure 12. The eigenvalues (E_i) of the transition matrix \mathbf{W} for the WT and the Dutch mutant peptides, expressed in units of ps^{-1} . The transition matrix \mathbf{W} , defined in eq. (10) has been calculated using the values of k_{ji} , obtained from the mean time τ_{ji} averaged over the four trajectories. The eigenvalues obtained from the simulation of the WT are presented as triangles, upper panel, those for the E22Q mutant peptide, as circles, lower panel.

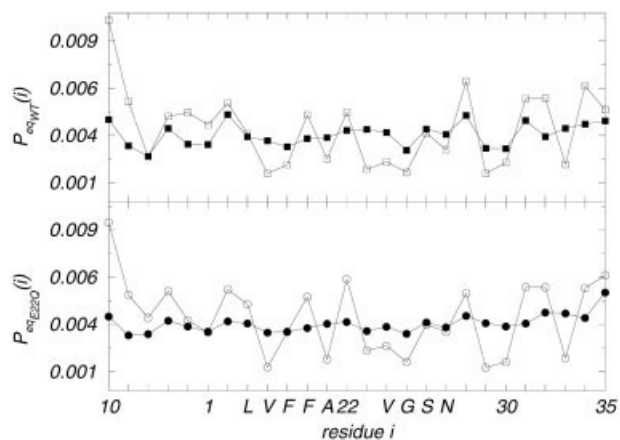


Figure 13. The probability distribution of water molecules around the peptide at equilibrium, for the WT, squares, and for the E22Q mutant peptide, circles. The equilibrium distributions obtained from the solution of the master equation, closed symbols, are compared with those computed directly from the trajectories, open symbols.

3. The hydrogen bond network between the solvent and the peptide is generally similar for both peptides. There is an anticorrelation between the formation of intramolecular hydrogen bonds and hydrogen bonds with the solvent. Those residues forming intramolecular peptide-peptide hydrogen bonds are in general less available to form hydrogen bonds with the solvent.
4. Residue D23 has a very high frequency of hydrogen bond formation, both with the atoms of the peptide and with the solvent. Relative to other residues, D23 is characterized by a significantly higher water residence time. The position of residue D23 along the peptide sequence is between the LVFFA and the VGSN turn regions, whose structures are the main motifs characterizing the conformation of the monomeric peptide in solution. The interaction between the sidechain of D23 and the solvent can have a strong influence on the structure and dynamics of the adjacent peptide residues, encouraging the formation of the turn region.
5. The eigenvalues that we obtained from the solution of the solvent relaxation master equation have a similar distribution in both peptide systems. Apart from the eigenvalue that is equal to zero, there is one of significantly smaller magnitude than all others. Some of the eigenvalues are complex, leading to an oscillatory behavior of $p_i(t)$ at short times. The time scale of the oscillatory part of the complex eigenvalues corresponds to that of the rapid recrossing of the solvation shell that we also found from calculating the water residence times. This observation may indicate that the ringing behavior found for $p_i(t)$ can be attributed to the process of rapid recrossing of water molecules near the boundary of the solvation shell.

In the early step of aggregation of monomeric peptides, once the peptides diffuse to contact, there will be a barrier to desolvation that must be overcome to create the peptide aggregate. Our analysis of the energetics and dynamics of the first hydration shell of

the peptide provides insights related to that desolvation process and its dependence on peptide sequence. All of our observations are consistent with the hypothesis that the E22Q mutant peptide presents a more flexible structure in solution, with greater hydrophobic surface area exposed to the solvent, and it has a weaker interaction with the water in the first solvation shell relative to the WT peptide.^{1,20} Our results suggest that, in the process of aggregation, the desolvation step can be energetically favored in the E22Q mutant over that in the WT peptide, in agreement with the increased activity of the Dutch mutant peptide.

Acknowledgments

J. E. S. gratefully acknowledges the Center for Computational Science at Boston University for essential computational resources. We thank Jonathan P. Lee for helpful comments.

References

- Massi, F.; Straub, J. E. *Biophys J* 2001, 81, 697.
- Selkoe, D. J. *J Neuropath Exp Neurology* 1991, 53, 438.
- Lansbury, P. T. Jr. *Acc Chem Res* 1996, 29, 317.
- Maggio, J. E.; Mantyh, P. W. *Brain Pathol* 1996, 6, 147.
- Teplow, D. B. *Amyloid: Int J Exp Clin Invest* 1998, 5, 121.
- Rochet, J.-C.; Lansbury, P. T. Jr. *Curr Opin Struct Bio* 2000, 10, 60.
- Lomakin, A.; Chung, D. S.; Benedek, G. B.; Kirschner, D. A.; Teplow, D. B. *Proc Natl Acad Sci USA* 1996, 93, 1125.
- Lomakin, A.; Teplow, D. B.; Kirschner, D. A.; Benedek, G. B. *Proc Natl Acad Sci USA* 1997, 94, 7942.
- Harper, J. D.; Wong, S. S.; Lieber, C. M.; Lansbury, P. T. Jr. *Chem Biol* 1997a, 4, 119.
- Walsh, D. M.; Lomakin, A.; Benedek, G. B.; Condron, M. M.; Teplow, D. B. *J Biol Chem* 1997, 272, 22364.
- Harper, J. D.; Wong, S. S.; Lieber, C. M.; Lansbury, P. T. Jr. *Chem Biol* 1997b, 4, 951.
- Esler, W. P.; Stimson, E. R.; Ghilardi, J. R.; Vinters, H. V.; Lee, J. P.; Mantyh, P. W.; Maggio, J. E. *Biochemistry* 1996, 35, 749.
- Kusumoto, Y.; Lomakin, A.; Teplow, D. B.; Benedek, G. B. *Proc Natl Acad Sci USA* 1998, 95, 12277.
- Zagorski, M. G.; Barrow, C. J. *Biochemistry* 1992, 31, 5621.
- Talafous, J.; Marcinowski, K. J.; Klopman, G.; Zagorski, M. G. *Biochemistry* 1992, 33, 7788.
- Shao, H.; Jao, S.-C.; Ma, K.; Zagorski, M. G. *J Mol Biol* 1999, 285, 755.
- Marcinowski, K. J.; Shao, H.; Clancy, E. L.; Zagorski, M. G. *J Am Chem Soc* 1998, 120, 11082.
- Esler, W. P.; Stimson, E. R.; Jennings, J. M.; Vinters, H. V.; Ghilardi, J. R.; Lee, J. P.; Mantyh, P. W.; Maggio, J. E. *Biochemistry* 2000, 39, 6288.
- Massi, F.; Straub, J. E. *Proteins* 2001, 42, 217.
- Zhang, S.; Iwata, K.; Lachenman, M. J.; Peng, J. W.; Li, S.; Stimson, E. R.; Lu, Y. A.; Felix, A. M.; Maggio, J. E.; Lee, J. P. *J Struct Biol* 2000, 130, 130.
- Barrow, C. J.; Yasuda, A.; Kenny, P. T.; Zagorski, M. G. *J Mol Biol* 1992, 225, 1075.
- Massi, F.; Peng, J. W.; Lee, J. P.; Straub, J. E. *Biophys J* 2001, 80, 31.
- Esler, W. P.; Felix, A. M.; Stimson, E. R.; Lachenmann, M. J.; Ghilardi, J. R.; Lu, Y.; Vinters, H. V.; Mantyh, P. W.; Lee, J. P.; Maggio, J. E. *J Struct Biol* 2000, 130, 174.
- Sian, A. K.; Frears, E. R.; El-Agnaf, O. A.; Patel, B. P.; Manca, M. F.; Siligardi, G.; Hussain, R.; Austen, B. M. *Biochem J* 2000, 349, 299.
- Melchor, J. P.; McVoy, L.; Van Nostrand, W. E. *J Neurochem* 2000, 74, 2209.
- Miravalle, L.; Chiarle, R.; Tokudand, T.; Giaccone, G.; Bugiani, O.; Ragliavini, F.; Frangione, B.; Ghiso, J. *J Biol Chem* 2000, 275, 27110.
- Watson, D. J.; Landers, A. D.; Selkoe, D. J. *J Biol Chem* 1997, 272, 31617.
- Zhang, S. Ph.D. Thesis, Boston University, Boston, MA, 1999.
- Kennedy, S. D.; Bryant, R. G. *Biopolymers* 1990, 29, 1801.
- Otting, G.; Lepinsh, E.; Wurthrich, K. *J Am Chem Soc* 1992, 114, 7093.
- Tominaga, Y.; Shida, M.; Kubota, K.; Urabe, H.; Nishimura, Y.; Tsuboi, M. *J Chem Phys* 1985, 83, 5972.
- Austin, R. H.; Roberson, M. W.; Mansky, P. *Phys Rev Lett* 1989, 62, 1912.
- Lindsay, S. M.; Powell, J. W.; Rupprecht, A. *Phys Rev Lett* 1984, 53, 1853.
- Teeter, M. M. *Annu Rev Biophys Chem* 1991, 20, 577.
- Hendrickson, W. A.; Teeter, M. M. *Nature* 1981, 290, 107.
- Cheng, X. D.; Schoenborn, B. P. *Acta Crystallogr B* 1990, 46, 195.
- Tao, N. J.; Rupprecht, S. M.; Lindsay, A. *Biopolymers* 1987, 26, 171.
- Grimm, H.; Stiller, H.; Majkrzak, C. F.; Rupprecht, A.; Dahlborg, U. *Phys Rev Lett* 1987, 59, 1780.
- Doster, W.; Cusack, S.; Petry, W. *Nature* 1989, 337, 754.
- Lee, J. P.; Stimson, E. R.; Ghilardi, J. R.; Mantyh, P. W.; Lu, Y.-A.; Felix, A. M.; Llanos, W.; Behbin, A.; Cummings, M.; Crieckinge, M. V.; Timms, W.; Maggio, J. E. *Biochemistry* 1995, 34, 5191.
- Mackerell, A. D. Jr.; Bashford, D.; Bellott, M.; Dunbrack, R. L. Jr.; Evanseck, J. D.; Field, M. J.; Fischer, S.; Gao, J.; Guo, H.; Ha, S.; Joseph-McCarthy, D.; Kuchnir, L.; Kuczera, K.; Lau, F. T. K.; Mattos, C.; Michnick, S.; Ngo, T.; Nguyen, D. T.; Prodhom, B.; Reiher, W. E. III; Roux, B.; Schlenkrich, M.; Smith, J. C.; Stote, R.; Straub, J. E.; Watanabe, M.; Wiokiewicz-Kuczera, J.; Yin, D.; Karplus, M. *J Phys Chem B* 1998, 102, 3586.
- Brooks, B. R.; Brucoleri, R.; Olafson, B.; States, D.; Swaminathan, S.; Karplus, M. *J Comp Chem* 1983, 4, 187.
- Garcia, A. E.; Stiller, L. *J Comput Chem* 1993, 14, 1396.
- Rocchi, C.; Bizzarri, A. R.; Cannistraro, S. *Chem Phys* 1997, 214, 261.
- Muegge, I.; Knapp, E. W. *J Phys Chem* 1995, 99, 1371.
- Simmerling, C.; Elber, R.; Zhang, J. In *Modelling of Biomolecular Structure and Mechanisms*; Pullman, A., Jortner, J., Pulman, B., Eds.; Kluwer: Netherlands, 1995; p 241.
- Rocchi, C.; Bizzarri, A.; Cannistraro, S. *Phys Rev E* 1998, 57, 3315.
- Bizzarri, A.; Cannistraro, S. *Phys Rev E* 1996, 53, 3040.
- Bizzarri, A.; Cannistraro, S. *Europhys Lett* 1997, 37, 201.
- Brooks, C. L.; Karplus, M. *J Mol Biol* 1989, 208, 159.
- Makarov, V. A.; Feig, M.; Andrews, B. K.; Pettitt, B. M. *Biophys J* 1998, 75, 150.
- Van Kampen, N. G. *Stochastic processes in physics and chemistry*; North-Holland: Amsterdam, 1992; pp 96–133.
- Wales, D. J.; Doye, J. P. K.; Miller, M. A.; Mortenson, P. N.; Walsh, T. R. In *Advances in chemical physics*, volume 115; Prigogine, I., Rice, S. A., Eds. John Wiley & Sons, Inc.: New York, 2000.
- Gardiner, C. W. *Handbook of stochastic methods*; Springer-Verlag: Germany, 1983.
- Hertz, H. G. In *Water: A comprehensive treatise*, Vol. 3; Franks, F., Ed.; Plenum Press: New York, 1973; pp 301–399.
- Knapp, E. W.; Muegge, I. *J Phys Chem* 1993, 97, 11339.
- Lounnas, V.; Pettitt, B. M.; Phillips, G. N. Jr. *Biophys J* 1994, 66, 601.
- Rosky, P. J.; Karplus, M. *J Am Chem Soc* 1979, 101, 1913.
- Zhang, S. S.; Casey, N.; Lee, J. P. *Fold Desg* 1998, 3, 413.
- Vertenstein, M.; Ronis, D. *J Chem Phys* 1987, 87, 5457.
- Wolynes, P. G. *Phys Rev A* 1976, 13, 1235.
- Cheng, Y. K.; Rosky, P. J. *Biopolymers* 1999, 50, 742.
- Cheng, Y. K.; Sheu, W. S.; Rosky, P. J. *Biophys J* 1999, 76, 1734.
- Carey, C.; Cheng, Y. K.; Rosky, P. J. *J Chem Phys* 2000, 258, 415.